Inverse Perovskites (RE_3N)Sn with RE = La, Ce, Pr, Nd, Sm: Preparation, Crystal Structures and Physical Properties

Martin Kirchner[a], Walter Schnelle[a], and Rainer Niewa[a,b]

[a] Max-Planck-Institut für Chemische Physik fester Stoffe, Nöthnitzer Straße 40, D-01187 Dresden, Germany
[b] Department Chemie, Technische Universität München, Lichtenbergstraße 4, D-85747 Garching, Germany

Reprint requests to Prof. Dr. R. Niewa. E-mail: rainer.niewa@ch.tum.de

Z. Naturforsch. **61b,** 813 – 819 (2006); received February 15, 2006

Dedicated to Professor Wolfgang Jeitschko on the occasion of his 70th birthday

The ternary compounds (RE_3N)Sn with RE = La, Ce, Pr, Nd, Sm were prepared starting from the elements. The compounds with RE = La, Ce, Pr were obtained as single phase materials according to X-ray powder diffraction patterns, which also indicate the cubic inverse perovskite crystal structure (space group $Pm\bar{3}m$, La: $a = 509.48(2)$ pm, Ce: $a = 501.59(2)$ pm, Pr: $a = 497.53(2)$ pm, Nd: $a = 494.70(5)$ pm, Sm: $a = 488.35(9)$ pm). Chemical analyses proof the correct composition and particularly the absence of nonmetallic constituents next to nitrogen. All studied compounds show metallic characteristics in the electrical resistivity. Magnetic susceptibility measurements indicate (La_3N)Sn to be a Pauli-paramagnet. Initially observed superconductivity was traced down to be due to thin La films on the surface of the grains. The Ce and Pr containing compounds show the behavior of $4f^1$ ions and $4f^2$ ions, and order antiferromagnetically at 6.8(2) K and 48(1) K, respectively.

Key words: Nitrides, Inverse Perovskites, Rare-Earth Metal Compounds, Magnetic Susceptibility, Electric Resistivity

Introduction

For metal-rich systems of alkaline-earth metals, or rare-earth metals RE with p group elements E, it has been established that many intermetallic compounds can accommodate nonmetallic elements in certain voids within the crystal structure. Depending on the system this can occur without significant changes of the host crystal structure and physical properties, with changes of physical properties and chemical and/or thermal stability, or with formation of a new compound or phase, of which the metal host structure is unknown in the respective binary intermetallic system. Interstitial elements are mostly Z = H, B, C, N, or O, but a large variety of elements, even transition metals, might be incorporated [1]. Apart from solution phases with only small amounts of a nonmetal component, with rare-earth metals only few different structure types dominate such systems. Most reports deal with $(RE_5Z_x)E_3$ and $(RE_3Z_x)E$ compositions, and of these the majority of the detailed investigations were carried out on carbides [2]. Phases of this general character with variable content of particularly Z = C, N, O dissolved in a host compound with little apparent structural effect have been designated "Nowotny phases" after the pioneering investigator of many examples in a variety of crystal structures, most frequently of transition metal silicides [3, 4]. Particularly carbides were intensively studied by Jeitschko for several decades, who also recently gathered the literature for perovskite carbides [5]. The lack of systematic and detailed studies on oxides and, in particular, nitrides is due to the fact, that these typically appear as impurity phases in the course of preparation experiments aimed at purely intermetallic compounds and due to the difficulty to specifically introduce the nonmetallic components N and O compared with C or B. Carbon, for example, can be added to an intermetallic melt bead simply in form of solid graphite.

In the binary systems RE–Sn, phases RE_3Sn were previously reported only for RE = La, Ce, Pr (although there was an unconfirmed claim of Gd_3Sn with an unknown crystal structure [6]). All three compounds were described to crystallize in the Cu_3Au structure

type [7, 8]. La_3Sn is under discussion since it does not appear in any phase diagram, but is reported to show superconductivity below temperatures of $T_c = 6.2$ K [9]. As frequent, the reports on La_3Sn may be due to unnoticed impurities of C, N, or O, as might be already indicated by the unit cell volumes. One report assigns La_3Sn a high-pressure phase. The unit cell parameter of a sample obtained at a pressure of $p = 7.5$ GPa ($a = 498(2)$ pm) is significantly smaller than those given in all other studies [10]. Ce_3Sn and Pr_3Sn were shown to decompose peritectically into a liquid phase and Ce_5Sn_3 ($T = 1210$ K) or Pr_5Sn_3 ($T = 1212$ K), respectively. On the basis of X-ray powder diffraction (no superstructure reflections indicating the primitive unit cell) and Mößbauer spectroscopic data (broad lines consistent with various surroundings of Sn) it was derived, that both compounds are substitutionally disordered, thus in a *ccp* arrangement rather than crystallizing in the Cu_3Au structure type [11]. However, different authors obtained Cu_3Au type Ce_3Sn ($a = 492.7$ pm) next to a cubic face-centered phase with larger unit cell dimensions ($a = 501$ pm). The latter phase again was interpreted as substitutionally disordered Ce_3Sn according to XRD and metallographic studies [12, 13]. Remarkably, the unit cell parameter of the disordered phase is nearly identical to the value obtained for (Ce_3N)Sn in the line of this work.

Only few ternary nitrides with Sn as a constituent are known. Previously reported were the inverse cubic perovskites (Ca_3N)Sn [14], (Sr_3N_{1-x})Sn, (Ba_3N_{1-x})Sn [15], (Nd_3N)Sn [16], (Cr_3N)Sn [17], (Mn_3N)Sn [17], (Mn_3N)$Mn_{0.5}Sn_{0.5}$ [18], and (Fe_3N)$Fe_{0.4}Sn_{0.6}$ [19], the filled Mn_5Si_3 type (Zr_3N)Zr_2Sn_3 [20] and the filled Cr_5B_3 type (La_4N)$LaPb_3$ [21]. Recently, the first nitridostannate(II) Na[SnN] was reported [22]. In the following, systematic investigations on phase formation, chemical and physical properties of the perovskites (RE_3N)Sn are reported.

Experimental Section

Since the rare-earth metals used as starting materials and the samples prepared are highly sensitive to air and moisture, all manipulations were carried out in argon-filled glove boxes (MBRAUN, $p(H_2O, O_2) < 1$ ppm).

The preparation of ternary compounds (RE_3N)Sn starts from high purity or purified rare-earth metal pieces as was described elsewhere [23] (Hunan Institute of Rare Earth Materials, 99.9% metal based). For production of nitride phases typically the binary nitride *RE*N was fused together with appropriate amounts of the respective binary alloys RE_2Sn in an arc-furnace. The resulting bead was wrapped in molybdenum foil, sealed in an evacuated quartz ampoule and annealed at elevated temperatures (typically $T = 1170$ K for several days).

Table 1. Lattice parameters and results of chemical analyses.

Compound	a [pm]	Chemical analysis	w(N) [wt.%]	w(O) [wt.%]
(La_3N)Sn	509.48(2)	($La_3N_{0.933(4)}O_{0.041(3)}$)Sn	2.38(1)	0.12(1)
(Ce_3N)Sn	501.59(2)	($Ce_3N_{1.027(4)}$)Sn	2.60(1)	< 0.10
(Pr_3N)Sn	497.53(2)	($Pr_3N_{0.899(4)}O_{0.049(7)}$)Sn	2.27(1)	0.14(2)
(Nd_3N)Sn	494.70(5)	not pure		
(Sm_3N)Sn	488.35(9)	not pure		

Chemical analyses on O, N and H were carried out on a LECO TCH 600 hot gas extractor. C was analyzed *via* combustion of the sample in oxygen on a LECO C 200. Detection limits typically were well below w(H,N,O) = 0.10%.

For X-ray diffraction the powdered samples were loaded between two Kapton-foils for protection from moisture and air. The X-ray experiments where carried out on an imaging plate Guinier-Camera (Huber-Diffraction, G 670) equipped with a quartz monochromator (Cu-$K_{\alpha 1}$-radiation, $6^\circ \leq \theta \leq 100^\circ$, 4×15 min).

Measurements of the magnetic susceptibilities were performed on a SQUID magnetometer (MPMS-XL7, Quantum Design) at fields between 2 mT and 7 T in the 1.8 K – 400 K range, using about 100 mg of single phase products sealed in a quartz tube under 400 mbar He.

Electrical resistivity measurements were performed on suitable pieces of the single phase products by a conventional dc four-point method between 3.5 K and 320 K. The contacts were made from silver-filled epoxy. All manipulations were carried out in an argon-filled glove box with an integrated cryostat for the resistance measurement.

Results and Discussion

Formation and stability

Regularly, the samples were characterized with XRD and chemical analyses. Table 1 gives unit cell parameters and results from chemical analyses. The unit cell parameters have been obtained from least-squares refinements of Guinier X-ray diffraction patterns. Chemical analyses on hydrogen and occasional checks for carbon indicated no such contaminations. The nitrides (La_3N)Sn, (Ce_3N)Sn, (Pr_3N)Sn, (Nd_3N)Sn, and (Sm_3N)Sn were successfully prepared, while no cubic perovskite nitrides could be obtained with RE = Sc, Gd, Lu. Together with the report on (Nd_3N)Sn from literature [16], this leads to the assumption, that nitrides

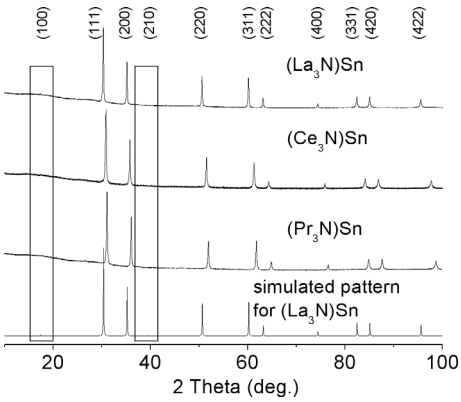

Fig. 1. Experimental XRD patterns of (La_3N)Sn (top), (Ce_3N)Sn (second), and (Pr_3N)Sn (third), together with the simulated pattern of (La_3N)Sn with a cubic perovskite crystal structure for comparison (bottom). The weak reflections at about 18 and 40 degrees 2Theta indicate the perovskite crystal structure in favor of a disordered cubic closed packed arrangement of the metal species. Miller indices are indicated.

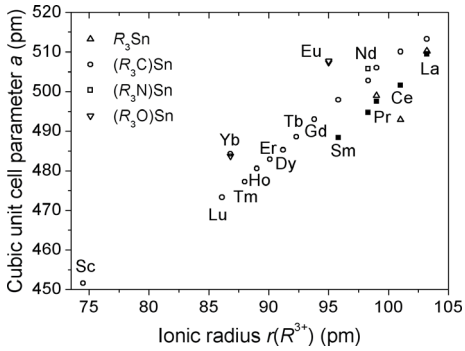

Fig. 2. Cubic unit cell parameter a for compounds (RE_3Z)Sn with $Z = \square$, C, N, O as a function of the radii of the rare-earth metal ions $r(RE^{3+})$ ($CN = 6$) [24], full symbols: this study, open symbols: literature data. Literature values were selected as discussed in the main text body [5, 7, 8, 16, 25 – 29].

do only form with the larger trivalent rare-earth metals with the border of formation located at Gd. Carbides, for comparison, exist for all rare-earth metals R.

Similar to the previous observations for the respective phases (RE_3N)In with indium as constituent [23], the binary compounds Ce_3Sn and Pr_3Sn show high macroscopic hardness paired with some ductility, while introduction of nitrogen leads to brittle compounds.

Crystal structure considerations

Fig. 1 shows the X-ray powder diffraction patterns of powdered samples (La_3N)Sn, (Ce_3N)Sn, and (Pr_3N)Sn in comparison to a simulated pattern for (La_3N)Sn with inverse cubic perovskite crystal structure. As in the case of compounds (RE_3N)In [23] only small differences in intensities as well as very weak superstructure reflections are produced by symmetry reduction from a hypothetical disordered sodium chloride type RE_3Sn and the proposed ordered occupation of octahedral holes leading to the final cubic perovskite type crystal structure.

Fig. 2 presents a plot of the cubic root of the cubic unit cell parameter a for the compounds (RE_3Z)Sn with $Z = \square$, C, N, O as a function of the ionic radii of the rare-earth metal ions in the oxidation state $+3$ ($CN = 6$) [24]. To ensure values from binary phases as pure as possible the smallest reported unit cells were chosen for the binary phases [7, 9, 25], while for the ternary phases the largest reported unit cells were selected, which are likely to contain the largest amounts of Z in the respective octahedral voids [5, 7, 8, 16, 25 – 29]. The unit cell parameter of Ce_3Sn significantly deviates from those of La_3Sn and Pr_3Sn to a smaller value, while the observed magnetic moment of μ_{eff}/Ce-atom $= 2.2\ \mu_{\text{B}}$ in Ce_3Sn is consistent with a $4f^1$ state (expected for Ce^{3+} free ion value: μ_{eff}/Ce-atom $\approx 2.5\ \mu_{\text{B}}$) [30]. This deviation of the unit cell dimension to smaller values than expected from those of the other compounds RE_3Sn was discussed to arise from substitutional disorder [11]. The carbides (RE_3C)Sn are known for all rare-earth metals $RE =$ Sc, La–Lu, except for $RE =$ Eu (and Pm) [5, 7, 8, 25, 29]. As can be taken from Fig. 2 the unit cell dimensions of the carbides with $R =$ La, Pr are only slightly larger than those reported for the binary compounds. The value for (Yb_3C)Sn clearly deviates from the monotonic behavior to a larger value, which might be interpreted as indication for a $Yb^{2+}(4f^{14})$ contribution. This view is supported by data on (Yb_3O)Sn [27], where the cubic unit cell parameter indicates the presence of primarily the $Yb^{2+}(4f^{14})$ state. Unfortunately, no information on physical properties of these Yb containing compounds was given. The cubic unit cell of the only previously known nitride (Nd_3N)Sn is even larger than that derived for (Nd_3C)Sn [16]. Except for (Yb_3O)Sn the only previously reported inverse perovskite oxide is (Eu_3O)Sn [26, 31].

The obtained values for the cubic unit cell parameters of the nitrides (Fig. 2) are well in correspondence with each other, while the previously reported data for (Nd_3N)Sn [16] strongly deviates towards a

larger value. This observation, together with the fact that the volume of the nitride is even larger than that of the corresponding carbide, may fuel speculations on a homogeneity range towards higher Sn contents. Striking are the smaller unit cell parameters of (La_3N)Sn and (Pr_3N)Sn compared with those of the respective binary compounds from literature, similar to what was observed for (Sc_3N)In compared to Sc_3In [23]. For the Sn containing phases this fact can not be related to different structure motifs of the metal constituents, as was discussed for the respective In systems. Apparently, the effect of attractive interactions between nitrogen and the metal constituents compensates the volume effect of the additional particle per formula unit.

Electronic properties

The magnetic properties of the (RE_3N)Sn compounds are dominated by the magnetic moment of the trivalent rare-earth ions *RE*.

The sample of (La_3N)Sn is weakly paramagnetic with a small field- and temperature-dependence of the susceptibility $\chi(T) = M(T)/H$ below *ca.* 300 K. The anomalous contribution probably originates from a minor ferromagnetic impurity ordering around this temperature. The size ΔM of this contribution corresponds to a Fe metal content of 25 ppm on mass. Using high-field data and correcting for this contribution it is found that (La_3N)Sn is a Pauli-paramagnet with a nearly temperature-independent susceptibility $\chi_0 = +140(20) \times 10^{-6}$ emu mol^{-1}. With the estimated sum of diamagnetic core contributions ($\chi_{\text{core}} \approx -89 \times 10^{-6}$ emu mol^{-1}) this yields $\chi_{\text{P}} = \chi_0 - \chi_{\text{core}} \approx 230 \times 10^{-6}$ emu mol^{-1}, corresponding to an electronic density of states of ≈ 7 states eV^{-1} at the Fermi level.

Susceptibility measurements $\chi(T)$ at low fields ($H_{\text{ext}} = 20$ and 100 Oe) recorded on microcrystalline pieces of (La_3N)Sn (Fig. 3) suggest superconductivity with $T_{\text{c}}(0) = 5.8(1)$ K. A shielding of 120% of the sample volume was measured on heating after zero-field cooling (zfc), but a very small Meissner effect ($\ll 1\%$ volume fraction) in field-cooling (fc) was found. Remarkably, the value of T_{c} almost coincides with the reported transition temperature of La_3Sn (Cu_3Au type structure) of $T_{\text{c}} = 6.2$ K [9]. The electrical resistivity *versus* temperature $\rho(T)$ of a piece of microcrystalline (La_3N)Sn (Fig. 4) is typical for a metal with $\rho(300\text{ K}) = 67\ \mu\Omega$ cm and $\rho_0 = 5\ \mu\Omega$ cm. With a current density $j = 3$ mA mm^{-2} at low temperatures

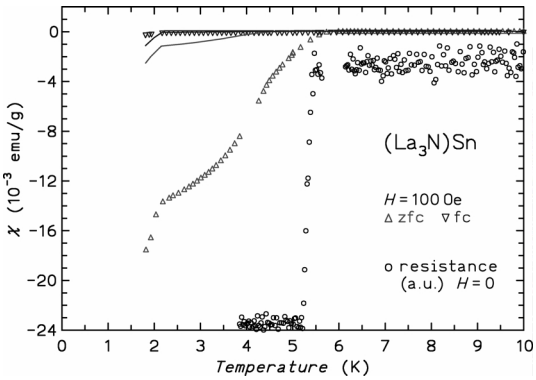

Fig. 3. (La_3N)Sn: Electrical resistance (black circles) and magnetic susceptibility of an as prepared sample (triangles). The observed superconductivity is most likely due to a thin La film (see text main body). Solid lines refer to fc (upper line) and zfc (lower line) susceptibility data of a ground powder.

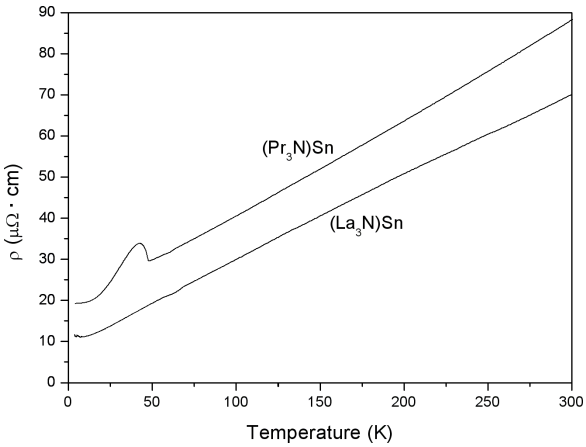

Fig. 4. Electrical resistivity of (La_3N)Sn and (Pr_3N)Sn as function of the temperature.

no superconductivity was detected above 3.8 K, only with $j = 0.75$ mA mm^{-2} a transition was observed at $T_{\text{c}} = 5.2$ K – 5.4 K. These observations give rise to two possible interpretations: i) (La_3N)Sn is a bulk superconductor with pinning (large difference of χ_{zfc} and χ_{fc}) but a very small critical current density (two obviously contradicting properties), or ii) the grains of the main phase (La_3N)Sn in the sample are covered with a thin layer of a superconducting secondary phase not visible in XRD (*e.g.*, elemental β-La, $T_{\text{c}} = 5.9$ K [32]). Susceptibility data $\chi(T)$ on identical sample material after grinding to a fine powder revealed only rudimentary remains of the diamagnetic shielding signal ($\chi_{\text{fc}}(T) \approx \chi_{\text{zfc}}(T)$); a strong support for the second interpretation.

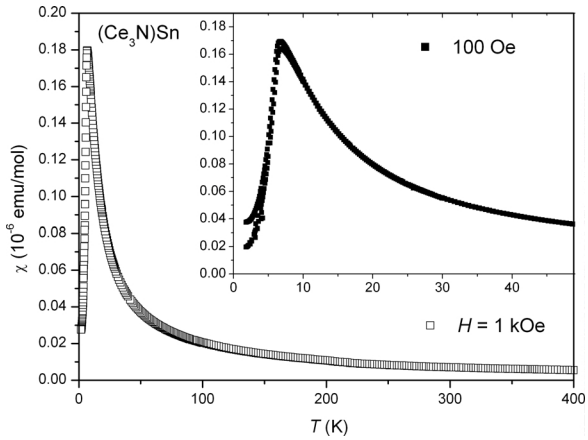

Fig. 5. Magnetic susceptibility *versus* temperature of (Ce_3N)Sn in a magnetic field of $H = 1$ kOe. The inset shows low-temperature data for $H = 100$ Oe.

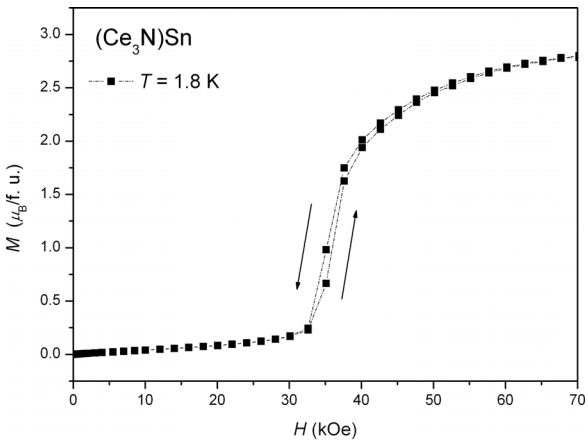

Fig. 6. Isothermal magnetization *versus* magnetic field for (Ce_3N)Sn at $T = 1.8$ K. The arrows indicate increasing and decreasing field direction.

(Ce_3N)Sn is a Curie-Weiss paramagnet displaying a susceptibility $\chi(T)$ (Fig. 5) in agreement with the properties of the $^2F_{5/2}$ crystal field ground multiplet of the $4f^1$ cerium ion (exclusive presence of Ce^{3+} ions). A linear fit of $1/\chi(T)$ in the temperature interval 100 K – 400 K leads to $\mu_{\mathrm{eff}}/\mathrm{Ce} = 2.46\ \mu_{\mathrm{B}}$, in good agreement with the free ion value (2.54 μ_{B}) [33], and $\Theta = -26$ K (afm). Thus, there is no indication for the presence of $4f^0$ ions in (Ce_3N)Sn. The $4f^1$ magnetic moments order antiferromagnetically at $T_{\mathrm{N}} = 6.8(2)$ K. This Néel temperature is of the same order as for (Ce_3N)In ($T_{\mathrm{N}} = 9.0$ K) [23].

Isothermal magnetization curves were recorded at 1.8 K, 3.0 K, 5.0 K, and 7.0 K up to fields $H_{\mathrm{ext}} =$ 70 kOe (Fig. 6). For the lowest measured temperature a metamagnetic transition starting above a field $H_{\mathrm{ext}} = 32$ kOe is observed. Here, the antiferromagnetic spin arrangement ($M = 0.2\ \mu_{\mathrm{B}}$/f.u. at 32 kOe) changes reversibly to a spin state with higher magnetization. Above $H_{\mathrm{ext}} = 38$ kOe the magnetization keeps on increasing and seems to saturate at $\approx 2.8\ \mu_{\mathrm{B}}$/f.u. at our maximum magnetic field of 70 kOe. This value is below the expected saturation magnetization of $3gJ \approx 3.7\ \mu_{\mathrm{B}}$ for 3 ions in the Γ_7 ground doublet of the $^2F_{5/2}$ state. With increasing temperature the jump in the magnetization is smeared out and moves to lower field values ($H_{\mathrm{ext}} \approx 24-33$ kOe for $T = 5$ K).

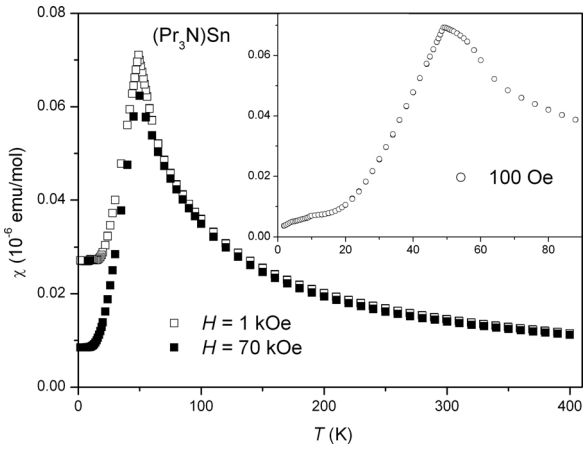

Fig. 7. Magnetic susceptibility *versus* temperature of (Pr_3N)Sn in a magnetic field of $H = 1$ kOe (open squares) and 70 kOe (full squares). The inset shows low-temperature data for $H = 100$ Oe.

The magnetic susceptibility $\chi(T)$ of polycrystalline (Pr_3N)Sn (Fig. 7) is fully compatible with the exclusive presence of the Pr^{3+} species ($4f^2$ ions with crystal field ground state multiplet $^3H_4$, free-ion moment 3.58 μ_{B}). A linear fit of a Curie-Weiss law to the (slightly negatively curved) data of $1/\chi(T)$ leads to $\mu_{\mathrm{eff}}/\mathrm{Pr} = 3.65\ \mu_{\mathrm{B}}$ and $\Theta = -50$ K. A clear cusp in $\chi(T)$ from an antiferromagnetic ordering of the Pr moments is visible at $T_{\mathrm{N}} = 49(1)$ K. This Néel temperature is much higher than that of (Pr_3N)In ($T_{\mathrm{N}} =$ 10.8 K) [23]), compatible with the smaller Pr–Pr distances due to the smaller unit cell of the Sn compound ($a = 497.53(2)$ pm) compared to the In compound ($a = 500.95(4)$ pm). Isothermal magnetization curves $M(H)$ at 2.0 K, 6.0 K and 14 K (Fig. 8) display all a small increase of $M(H)$ for the ordered spin structure (only $0.11-0.12\ \mu_{\mathrm{B}}$/f.u. at 70 kOe) and for $T = 2.0$ K a weak metamagnetic transition between 8 kOe and 1.2 kOe.

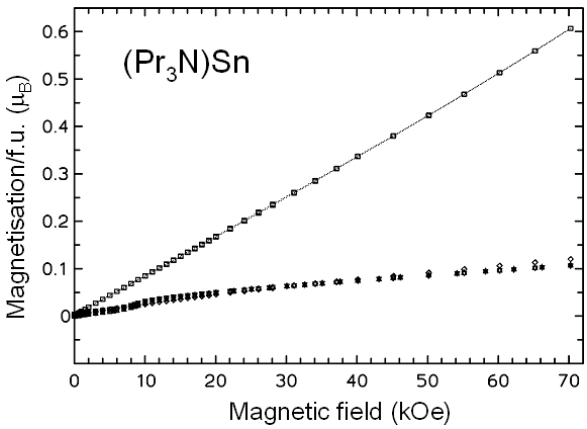

Fig. 8. Isothermal magnetization curves *versus* magnetic field of (Pr_3N)Sn at $T = 2.0$ K (triangles, the orientation of the symbols indicate the field sweep directions), $T = 6.0$ K (circles), $T = 14.0$ K (diamonds), $T = 40.0$ K (squares).

The electrical resistivity $\rho(T)$ of a piece of microcrystalline (Pr_3N)Sn (Fig. 4) is linear at high temperatures ($\rho(300\text{ K}) = 19\ \mu\Omega\,\text{cm}$, $\rho_0 = 88\ \mu\Omega$ cm) and typical for a metallic state. The antiferromagnetic ordering of the $4f^2$ moments is signalled by a sharp kink in $\rho(T)$ at 48(1) K. The relatively strong rounded peak in $\rho(T)$ below T_N is uncommon. Usually, $\rho(T)$ decreases strongly below T_N due to the drastically weaker scattering of the conduction electrons on the ordered magnetic moments. A relative increase of $\rho(T)$ around T_N might be due to critical effects which, however, should show up as a (positive) cusp in $\rho(T)$ exactly at T_N.

Conclusions

In combination with rare-earth elements Sn forms cubic perovskite nitrides with metallic properties, similar to other main group elements from the *p*-block of the periodic table like, *e. g.*, Al or In, and similar to the respective carbides. However, with Gd and heavier rare-earth elements no such ternary nitrides could be obtained. Electronic properties as, *e. g.*, the magnetic behavior connects to the known compounds with trivalent rare-earth metal constituents: The La compound shows temperature independent paramagnetism. A transition to a superconducting state was traced down to thin La impurity layers on the surface of the initial grains. The Ce and Pr compounds order antiferromagnetically and the transition temperature scales with the magnetic moment and the distance *RE*–*RE*, which can be influenced by the nature of the nonmetallic element – in the presented work set to nitrogen.

Acknowledgements

We thank Steffen Hückmann for the collection of the diffraction data, Anja Völzke for performing the chemical analyses, Ralf Koban for operating the SQUID and preparing the resistivity measurements, and Prof. Dr. R. Kniep for his constant interest and support.

[1] J. D. Corbett, E. Garcia, A. M. Guloy, W.-M. Hurng, Y.-U. Kwon, A. E. Leon-Escamilla, Chem. Mater. **10**, 2824 (1998).
[2] G.-Y. Adachi, N. Imanaka, Z. Fuzhong, in K. A. Gschneidner (Jr.), L. Eyring (eds): Handbook on the Physics and Chemistry of Rare Earths, Vol. 15, Elsevier, Amsterdam (1991).
[3] H. Nowotny, Alloy Chemistry of Transition Element Borides, Carbides, Nitrides, Aluminides and Silicides, in P. A. Beck (ed.): Electronic Structure and Alloy Chemistry of the Transition Elements, pp. 179, Interscience Publishers, New York (1963).
[4] R. Kieffer, F. Benesowsky, B. Lux, Planseeber. Pulvermetall. **4**, 30 (1956).
[5] T. M. Gesing, K. H. Wachtmann, W. Jeitschko, Z. Naturforsch. **52b**, 176 (1997).
[6] L. Qu Jing, Z. Jian Xuan, C. S. Cheng, Acta Physica Sinica **33**, 1155 (1984).
[7] W. Jeitschko, H. Nowotny, F. Benesovsky, Monatsh. Chem. **95**, 1040 (1964).
[8] H. Haschke, H. Nowotny, F. Benesovsky, Monatsh. Chem. **97**, 1045 (1966).
[9] C. S. Garde, J. Ray, G. Chandra, J. Alloys Compd. **198**, 165 (1993).
[10] V. I. Larchev, S. V. Popova, Sov. Phys. Solid State **19**, 852 (1977).
[11] I. J. McColm, N. J. Clark, B. Mortimer, J. Inorg. Nucl. Chem. **33**, 49 (1971).
[12] E. A. Franceschi, G. A. Costa, J. Thermal Analysis **34**, 451 (1988).
[13] G. Borzone, A. Borsese, R. Ferro, J. Less-Common Met. **85**, 195 (1982).
[14] M. Y. Chern, D. A. Vennos, F. J. DiSalvo, J. Solid State Chem. **96**, 415 (1992).
[15] F. Gäbler, M. Kirchner, W. Schnelle, M. Schmitt, H. Rosner, R. Niewa, Z. Anorg. Allg. Chem. **631**, 397 (2005).
[16] H. Haschke, H. Nowotny, F. Benesovsky, Monatsh. Chem. **98**, 2157 (1967).
[17] M. Nardin, G. Lorthioir, M. M. Barberon, R. Madar,

E. Fruchart, R. Fruchart, Compt. Rend. Hebd. Acad. Sci. C **274** 2168 (1972).
[18] M. Mekata, J. Phys. Soc. Jpn. **17**, 796 (1962).
[19] Z. J. Zhao, D. S. Xue, F. S. Li, J. Magn. Magn. Mater. **232**, 155 (2001).
[20] K. Young-Uk, J. D. Corbett, Chem. Mater. **4**, 1348 (1992).
[21] A. M. Guloy, J. D. Corbett, Z. Anorg. Allg. Chem. **616**, 61 (1992).
[22] N. S. P. Watney, Z. A. Gal, M. D. S. Webster, S. J. Clarke, Chem. Commun. **33**, 4190 (2005).
[23] M. Kirchner, W. Schnelle, F. R. Wagner, R. Niewa, Solid State Sci. **5**, 1247(2003).
[24] R. D. Shannon, Acta Crystallogr. **A32**, 751 (1976).
[25] H. Haschke, H. Nowotny, F. Benesovsky, Monatsh. Chem. **97**, 716 (1966).
[26] R. Türck, Ph D Thesis, Universität Stuttgart, Germany (1996).
[27] A. Velden, M. Jansen, Z. Anorg. Allg. Chem. **630**, 234 (2004).
[28] H. Hollek, J. Less-Common Met. **52**, 167 (1977).
[29] H. Haschke, H. Nowotny, F. Benesovsky, Monatsh. Chem. **97**, 1469 (1966).
[30] F. Weitzer, K. Hiebl, P. Rogl, J. Less-Common Met. **175**, 331 (1991).
[31] M. Kirchner, W. Schnelle, R. Niewa, Z. Anorg. Allg. Chem. **632**, 559 (2006).
[32] A. L. Griorgi, E. G. Szklarz, M. C. Krupta, N. H. Krikorian, J. Less-Common Met. **17**, 121 (1969).
[33] H. Lueken, Magnetochemie, B. G. Teubner, Stuttgart (1999).